Self-propelled cavity solitons in semiconductor microcavities

A. J. Scroggie,* J. M. McSloy,† and W. J. Firth‡
Department of Physics and Applied Physics, University of Strathclyde, 107 Rottenrow, Glasgow G4 ONG, Scotland
(Received 19 April 2002; published 19 September 2002)

We demonstrate the existence of both bright and dark spontaneously moving spatial solitons in a model of a semiconductor microcavity. The motion is caused by temperature-induced changes in the cavity detuning and arises through an instability of the stationary soliton solution above some threshold. An order parameter equation is derived for the moving solitons and is used to explain their behavior in the presence of externally imposed parameter modulations. The existence of two-dimensional moving solitons is demonstrated and an example given of their interaction.

DOI: 10.1103/PhysRevE.66.036607 PACS number(s): 05.45.Yv, 42.65.Tg, 42.55.Px

I. INTRODUCTION

Optical cavities containing nonlinear media provide all the ingredients necessary for the observation of dissipative structures: losses, external driving, nonlinearity, and spatial coupling. One interesting and common type of solution is spatial solitary waves (cavity solitons), localized bright, or dark spots in the plane transverse to the direction of propagation of the optical field. Such structures have been predicted in a variety of systems and also observed experimentally. For recent reviews see [1,2].

When the driving field is a plane wave and the system invariant with respect to spatial translations, the soliton can exist at any location. Motion can be induced by breaking the translational symmetry with the imposition of a spatial modulation on a parameter, such as the pump phase or amplitude [3,4] or the cavity detuning. In this paper we describe, instead, a spontaneous transition from stationary to moving solitons, through a bifurcation of the system. This is made possible by turning one of the parameters (here, the detuning) into a dynamical variable. The physical motivation is the inclusion of thermal effects in our system—a semiconductor microcavity. Moving solitons have been reported in simulations of an alternative model of the same system [5], which includes a very detailed form of semiconductor nonlinearity. Our discovery of the same phenomenon in a much simpler model allows an investigation of the nature of the solutions and the instability which gives rise to them. We note that the stationary-to-moving soliton bifurcation has similarities with the Ising-Bloch transition studied in [6] and more recently in [7,8]. One notable feature of the present system, however, is the existence of a clear physical interpretation for the motional instability.

In Sec. II we will introduce our system and the model used to describe it. Section III will analyze moving solitons in one spatial dimension. The existence and interaction of moving solitons in two dimensions will be demonstrated briefly in Sec. IV. Finally, Sec. V contains some conclusions.

*Electronic address: andrew@phys.strath.ac.uk
†Electronic address: jmc@phys.strath.ac.uk
‡Electronic address: willie@phys.strath.ac.uk

II. THE MODEL

The system under consideration is a semiconductor microcavity (Fig. 1) consisting of an active region sandwiched between two high reflectivity ($\sim$99.9%) distributed Bragg reflectors (DBR). The device is driven by an external pump field E_I and, optionally, an external current J. When J is less than some threshold value J_0 the semiconductor medium acts as an absorber, while for J greater than J_0 it behaves as an amplifier. If the current is sufficiently large to cause the gain in the semiconductor to exceed the cavity losses, the system will lase.

The intracavity electric field E, carrier density N, and temperature difference T between the lattice temperature and the ambient temperature can be described by the following set of partial differential equations [5,9,10]:

$$\frac{\partial E}{\partial t} = -(1+i\Theta)E + i\Xi\chi E + E_I + i\nabla_\perp^2 E, \tag{1}$$

$$\frac{\partial N}{\partial t} = -\gamma_N[N+\beta N^2 - J + (N-1)|E|^2 - D_N\nabla_\perp^2 N], \tag{2}$$

$$\frac{\partial T}{\partial t} = -\gamma_T(T - ZN - PJ^2 - D_T\nabla_\perp^2 T), \tag{3}$$

where $\nabla_\perp^2$ is the transverse Laplacian $\partial_x^2+\partial_y^2$. These equations apply to both an amplifying (active) device and a pas-

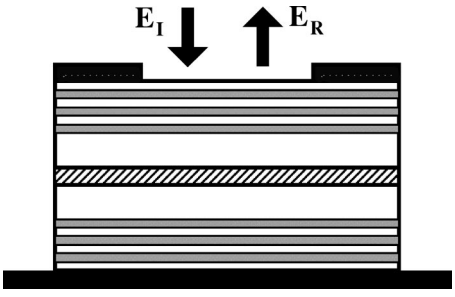

FIG. 1. Illustration of an externally driven semiconductor microcavity. The central cross-shaded area represents the active region which is sandwiched between spacers (shown in white). The striped regions are the distributed Bragg reflectors and black bars denote electrical contacts.

sive multiple-quantum well (MQW) device. The strength of the material nonlinearity is parametrized by Ξ. The cavity detuning is denoted by Θ where

$$\Theta = \theta - \alpha T, \tag{4}$$

with θ being the cavity detuning at ambient temperature and α a coupling parameter [11]. Equation (4) embodies the most important consequence of heating in semiconductor microcavity devices: namely, a change in the linear refractive index of the semiconductor material and hence a shift in the cavity resonances [11,12].

The normalization of the carrier density has been chosen so that the critical current J_0 is equal to unity. The term βN^2 describes radiative carrier recombination. Carrier and thermal diffusion coefficients [13] are denoted by D_N and D_T.

The fields E, N, and T decay on time scales of $\tau \sim 10$ ps (the cavity lifetime), $\gamma_N^{-1} \sim 1$ ns and $\gamma_T^{-1} \sim 1$ μs, respectively. The nonlinear susceptibility χ is assumed to be simply a linear function of the carrier density:

$$\chi = -(\Delta + i)(N-1) \quad \text{(active device)}, \tag{5}$$

$$\chi = \frac{-(\Delta + i)(N-1)}{1+\Delta^2} \quad \text{(passive MQW device)}. \tag{6}$$

The parameter Δ represents the linewidth enhancement factor for an active device and the band-gap detuning for a passive device. Note that this form of the susceptibility in the passive device implies a detuning-dependent scaling of the electric field:

$$F \propto E\sqrt{1+\Delta^2}, \tag{7}$$

where F is the unscaled electric field.

Finally, the terms ZN and PJ^2 describe heating due to nonradiative recombination and Joule heating from the injection current, respectively.

Equations (1)–(3) are known to exhibit plane-wave bistability and to possess stable, stationary soliton solutions in the absence of thermal effects ($\alpha = 0$) [4]. Below we describe new structures whose existence is due entirely to the effect of temperature changes on the cavity and thereby on the intracavity field.

III. ONE-DIMENSIONAL MOVING CAVITY SOLITONS

A. Active configuration

Modulation of parameters such as the pump field or cavity detuning is generally expected to induce movement in cavity solitons [3,4]. The movement arises from a nonzero projection of the parameter modulation onto the neutral mode of the unperturbed system. This neutral mode corresponds to the generator of translations and therefore driving it produces a change in the position of the soliton [4]. In the present model, the detuning is not a parameter but, through the temperature, a dynamical variable, capable of spontaneous spatial variation. This creates the right circumstances for the existence of spontaneously moving solitons.

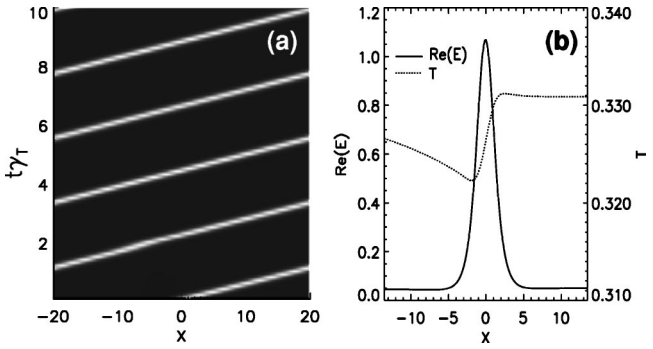

FIG. 2. (a) Space-time plot of the real part of the electric field for a moving soliton. (b) Electric field and temperature components of a moving soliton. $E_I = 0.350$, $\alpha = 3.0$, $D_N = 0.052$, $D_T = 1$, $\gamma_N = 10^{-2}$, $\gamma_T = 10^{-5}$, $\Delta = 5$, $\theta = -2$, $\Xi = 0.9$, $J = 2$, $\beta = 0$, $Z = 0.172$, $P = 1.2 \times 10^{-4}$.

Equations (1)–(3) were integrated numerically in one spatial dimension on a grid of anywhere between 256 and 1024 points using a split-step method [14]. Figure 2 shows an example of a moving soliton. The movement can be thought of as arising from an instability of the stationary soliton which, for an amplifier, has a temperature minimum at its center. When the peak of the optical intensity is displaced from the temperature minimum, it lowers the temperature at its new location, but also moves in the detuning gradient on which it finds itself. If the movement is slow enough for the temperature to respond, the soliton just establishes itself at a new location. If, however, the effect of the gradient (controlled by the parameter α [Eq. (4)]) is large enough, the intensity peak will keep moving, cooling the material it meets while the temperature relaxes to the ambient level behind it, in a process which sustains the detuning gradient, and therefore the motion. From the symmetry of the problem, there are clearly two such moving solutions, one in each direction in space. This argument clearly requires that the temperature gradient is such as to make the soliton move away from, not towards, its original position.

Figure 3 shows stationary and moving soliton branches as a function of the pump amplitude E_I, for several different values of α, the coupling strength between optical field and temperature. The stationary solutions, even though unstable, can be computed to arbitrary precision using a relaxation method [15]. While the two solution branches are disjoint for large values of α, their merging as α decreases is evident and suggests that the moving solutions emerge from a (supercritical) bifurcation of the stationary solitons. In fact, as implied above, α is the most natural parameter to use when describing this bifurcation. The appearance of the moving solution is most easily analyzed by studying the stability of the stationary solution via the eigenvalues of the Jacobian. These eigenvalues and the corresponding eigenvectors can be calculated numerically, again to high accuracy [15].

Figure 4 plots the nonzero eigenvalue with largest real part (corresponding to the motional instability) as a function of α, for a fixed pump value of $E_I = 0.770$. The instability occurs at $\alpha \simeq 0.039$, when the eigenvalue becomes positive. Figure 5 shows an example of an unstable eigenfunction, as

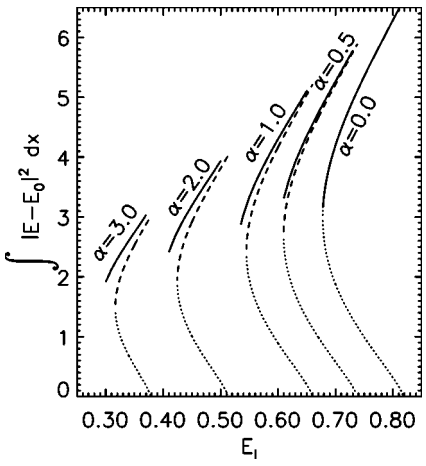

FIG. 3. Stationary (dashed and dotted lines) and moving (solid lines) soliton solution branches as functions of the external pump amplitude. The curves correspond to values of α of (from left to right) 3.0, 2.0, 1.0, 0.5, and 0. All other parameters are as in Fig. 2. Each solution on the dotted stationary branch is unstable to the corresponding solution on the dashed branch, as well as to the moving solution. The quantity E_0 in the vertical axis label denotes the background solution on which the soliton sits.

well as the null eigenfunction which arises from the translational invariance of the system and which is proportional to the spatial derivative of the fields. The temperature components of the eigenfunctions are clearly different while the components corresponding to the real part of the electric field are very similar (as are those for the imaginary part of the field and for the carrier density). This reflects the fact that the instability alters the temperature profile and drives the motion of the optical field and carrier density. Figure 6 shows a space-time plot of a stationary soliton becoming unstable to a moving soliton.

From similar stationary-to-moving bifurcations [6,7], or simply from continuity, the velocity of the moving solution should go to zero as the bifurcation point is approached from

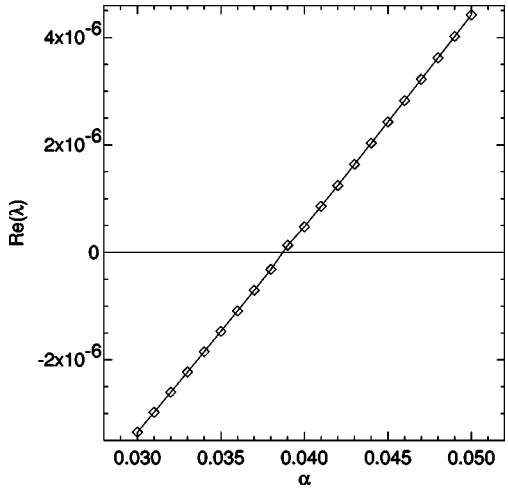

FIG. 4. The eigenvalue λ which leads to the motional instability as a function of α.The imaginary part of λ is always zero. $E_I = 0.770$, all other parameters as in Fig. 2.

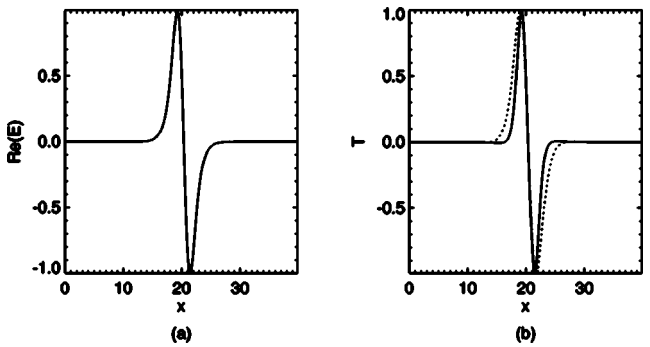

FIG. 5. The electric field and temperature components of the unstable mode (solid line) and the neutral mode (dashed line) of the stationary soliton solution. In panel (a) the two functions effectively coincide. All parameters as in Fig. 2; in particular, $\alpha = 3.0$ and $E_I = 0.35$.

above (Fig. 7) and the stationary and moving solutions coincide. At the bifurcation point the unstable eigenfunction is then identical to the null eigenfunction. This degeneracy has important consequences for the behavior of the moving solitons in the presence of externally imposed perturbations, as we will see in Sec. III C.

Since the moving solutions depend upon a balance between the relaxation rate of the temperature and the response of the optical field to a detuning gradient, increasing the value of the thermal time constant γ_T should increase the value of α at which the instability appears. Figure 8 confirms this, showing that an increase in γ_T from 10^{-5} to 10^{-4} requires an increase in α of roughly an order of magnitude before the moving solitons appear. This is relevant for experiments, given the uncertainty in the values of this and the other thermal parameters [12].

B. Passive configuration

The instability to moving solutions described in the preceding section can also be observed for dark solitons in the passive system. This is consistent with the mechanism de-

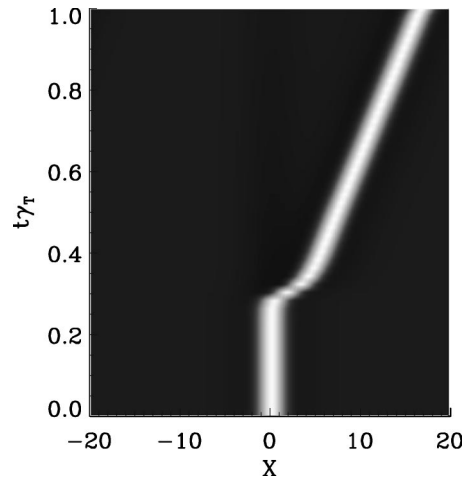

FIG. 6. Space-time plot of the destabilization of a stationary soliton to a moving soliton. All parameters as in Fig. 2.

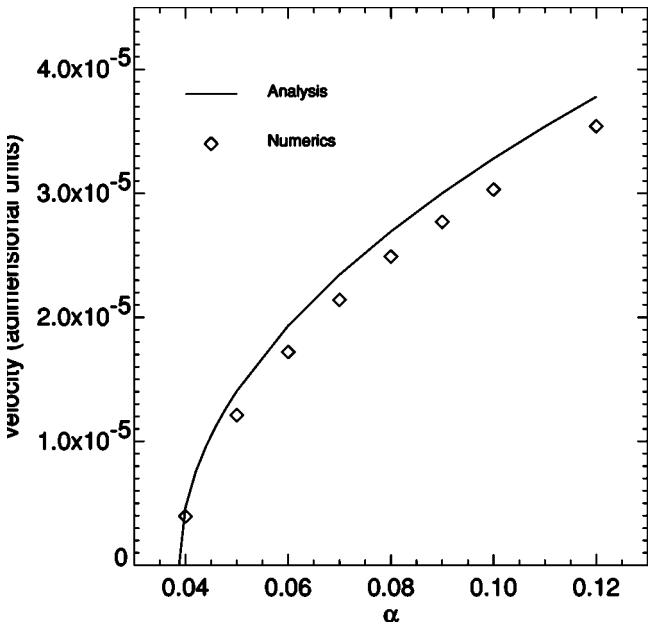

FIG. 7. The velocity of a moving soliton as a function of α. All parameters as in Fig. 4. The diamonds indicate results from numerical simulations. The solid line comes from weakly nonlinear analysis (see Sec. III C).

scribed above, since a passive medium is cooled by a dark soliton, just as an active one is by a bright soliton.

As intensity minima sitting on a high-intensity background, dark solitons are expected to exist on the upper branch of the plane-wave bistability curve. Figure 9 shows an example of a dark soliton branch along with plane-wave and roll solutions. The roll solution has a wave vector $K \simeq 1.3K_c$ where K_c is the most unstable wave vector at the modulational instability threshold. In contrast with Fig. 3, the homogeneous background field has not been subtracted from the soliton field, in order to show the underlying plane-wave

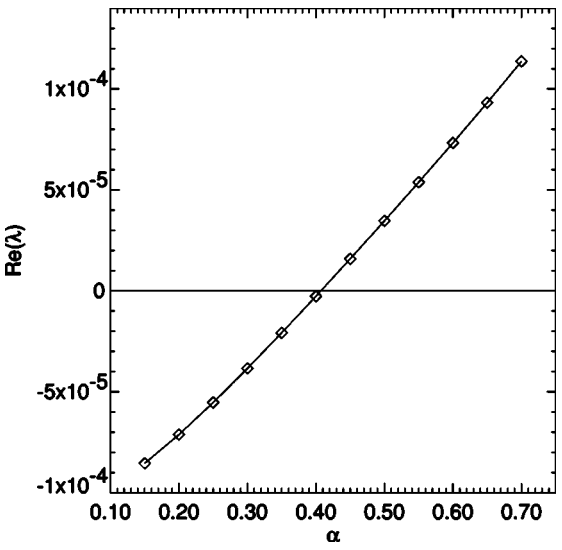

FIG. 8. The eigenvalue λ which leads to the motional instability as a function of α and for $\gamma_T = 10^{-4}$. All other parameters as in Fig. 4.

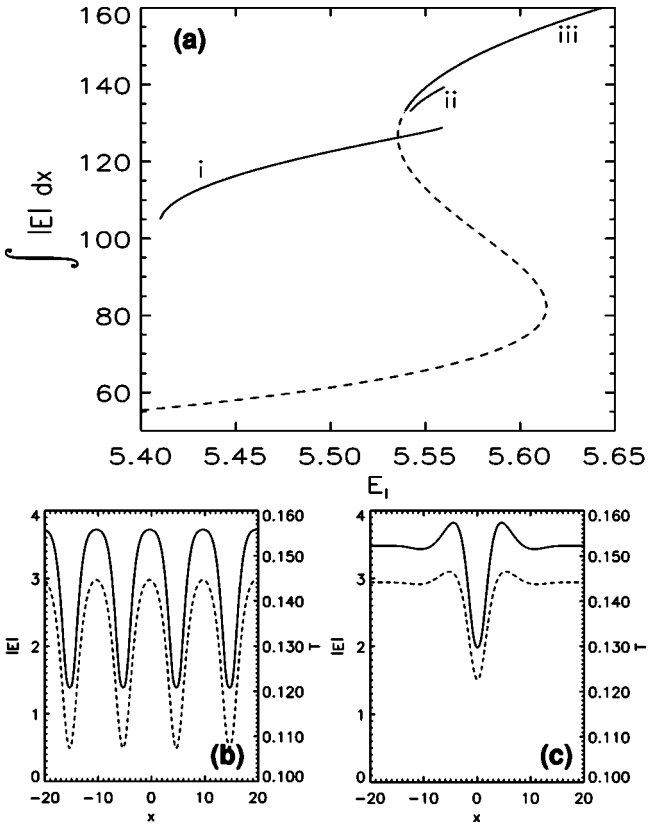

FIG. 9. (a) Solution branches for (i) rolls with $K \simeq 1.3K_c$ and (ii) stationary dark solitons. Panels (b) and (c) correspond, respectively, to points on branches (i) and (ii). Solid and dashed lines, respectively, denote $|E|$ and T. The homogeneous solution (iii) is stable on solid parts of the curve and modulationally unstable in the dashed region. Parameters are $\alpha = 1$, $D_N = 0.2$, $D_T = 1$, $\gamma_N = 10^{-2}$, $\gamma_T = 10^{-5}$, $\Delta = 10$, $\theta = 0.3$, $\Xi = 80$, $\beta = 1.6$, $Z = 0.172$. (b) $E_I = 5.45$ and (c) $E_I = 5.55$.

bistability. For these parameters, dark solitons exist for $5.542 < E_I < 5.560$ but are always unstable to spontaneous motion. An example of a moving dark soliton is given in Fig. 10. As in the active case the translational modes of the electric field and carrier density are driven by the temperature gradient.

Moving solitons, whether in the active or passive system, rely on a local increase in the cavity detuning which, for

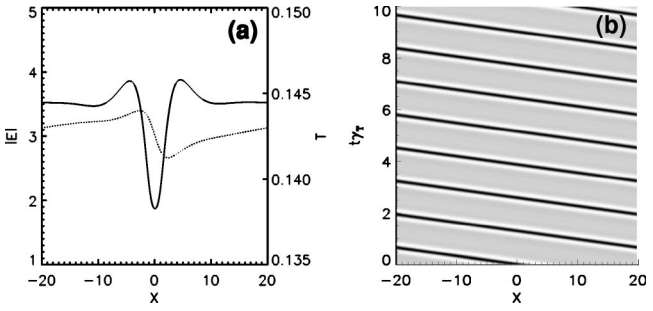

FIG. 10. (a) Magnitude of electric field (solid line) and temperature (dotted line) for a dark moving soliton. (b) Space-time plot of a moving soliton. Parameters are $E_I = 5.39$ and $\alpha = 1$. All other parameters as in Fig. 9.

positive α, is caused by a local cooling of the medium. If, instead, we consider a system in which α is negative, such an effect will be produced by locally heating the medium. In that case, dark and bright moving solitons should exist in active and passive systems, respectively, in contrast with the semiconductor cavity considered here.

C. Soliton equation of motion

We can perform a weakly nonlinear analysis near the bifurcation point between the stationary and moving solutions. The calculation has similarities to that reported in [8].

We first define

$$\mathbf{V}=[E,E^*,N,T]^T=\mathbf{V}_0+\mathbf{W}, \tag{8}$$

where $\mathbf{V}_0=[E_0,E_0^*,N_0,T_0]^T$ is the stationary soliton solution. In addition, we change co-ordinates to t and $\xi=x-vt$, where v is the (unknown) soliton velocity, to obtain an equation of the following form for $\mathbf{W}$:

$$\partial_t\mathbf{W}=\mathcal{L}\mathbf{W}+\mathbf{N}(\mathbf{W})+v(\partial_\xi\mathbf{W}+\partial_\xi\mathbf{V}_0). \tag{9}$$

The operator $\mathcal{L}$ is a linear operator, whose form at the bifurcation point is denoted by $\mathcal{L}_0$, while $\mathbf{N}$ is nonlinear. Before proceeding we note that, since the mode giving rise to the instability coincides with $\boldsymbol{\phi}_0$, the null eigenvector of $\mathcal{L}_0$, the eigenvectors of $\mathcal{L}_0$ do not form a basis for the space. The set can be completed by $\boldsymbol{\psi}_0$, the null eigenvector of $\mathcal{L}_0^\dagger$, which is orthogonal to *all* eigenvectors of $\mathcal{L}_0$. In addition, there exists a generalized eigenvector [16] $\boldsymbol{\phi}_c$, which will be important in the following analysis and which satisfies the equation

$$\mathcal{L}\boldsymbol{\phi}_c=-\boldsymbol{\phi}_0. \tag{10}$$

We now introduce a smallness parameter ε and expand all relevant quantities in appropriate powers of ε:

$$\begin{aligned}\mathbf{W}&=\varepsilon\mathbf{W}_1+\varepsilon^2\mathbf{W}_2+\varepsilon^3\mathbf{W}_3+\cdots,\\ \mathcal{L}&=\mathcal{L}_0+\varepsilon^2\mathcal{L}_2,\\ \partial_t&=\varepsilon^2\partial_\tau,\\ v&=\varepsilon\mu.\end{aligned} \tag{11}$$

Collecting terms order by order in ε we find at $O(\varepsilon)$

$$\mathcal{L}_0\mathbf{W}_1=-\mu\boldsymbol{\phi}_0, \tag{12}$$

whose solution, from Eq. (10), is

$$\mathbf{W}_1=\mu\boldsymbol{\phi}_c. \tag{13}$$

The quantity μ appears as an unknown multiplier of the unstable eigenvector $\boldsymbol{\phi}_c$ and we expect the subsequent analysis to yield equations governing its dynamics. In other words, μ (or the velocity) is the order parameter of the system.

At $O(\varepsilon^2)$

$$\mathcal{L}_0\mathbf{W}_2=-\mathbf{N}_2(\mathbf{W})-\mu^2\partial_\xi\boldsymbol{\phi}_c\equiv\mathbf{S}_2, \tag{14}$$

where $\mathbf{N}_2(\mathbf{W})$ denotes the nonlinear terms of second order in ε. Because $\mathcal{L}_0$ is singular, $\mathbf{S}_2$ must be orthogonal to $\boldsymbol{\psi}_0$ for a solution to exist. Since $\boldsymbol{\psi}_0$ is an odd function of ξ, while all terms in $\mathbf{S}_2$ are even, the inner product $(\boldsymbol{\psi}_0,\mathbf{S}_2)$ is automatically zero and at least one solution exists for $\mathbf{W}_2$.

At $O(\varepsilon^3)$

$$\begin{aligned}\mathcal{L}_0\mathbf{W}_3&=\partial_\tau\mathbf{W}_1-\mathcal{L}_2\mathbf{W}_1-\mathbf{N}_3(\mathbf{W})-\mu\partial_\xi\mathbf{W}_2\\ &=(\partial_\tau\mu)\boldsymbol{\phi}_c-\mu\mathcal{L}_2\phi_c-\mu^3\mathbf{n}_3(\mathbf{W})-\mu^3\partial_\xi\mathbf{w}_2\\ &\equiv\mathbf{S}_3,\end{aligned} \tag{15}$$

where $\mathbf{N}_3(\mathbf{W})$ denotes the nonlinear terms of third order in ε and

$$\begin{aligned}\mathbf{N}_3(\mathbf{W})&\equiv\mu^3\mathbf{n}_3(\mathbf{W}),\\ \mathbf{W}_2&\equiv\mu^2\mathbf{w}_2;\end{aligned} \tag{16}$$

that is, the order parameter μ has been factored out of $\mathbf{N}_3$ and $\mathbf{W}_2$. Again, $(\boldsymbol{\psi}_0,\mathbf{S}_3)$ must be zero for a solution to exist, which implies (undoing the scalings)

$$\partial_t v=\frac{(\boldsymbol{\psi}_0,[\mathcal{L}-\mathcal{L}_0]\boldsymbol{\phi}_c)}{(\boldsymbol{\psi}_0,\boldsymbol{\phi}_c)}v+\left[\frac{(\boldsymbol{\psi}_0,\mathbf{n}_3)}{(\boldsymbol{\psi}_0,\boldsymbol{\phi}_c)}+\frac{(\boldsymbol{\psi}_0,\partial_\xi\mathbf{w}_2)}{(\boldsymbol{\psi}_0,\boldsymbol{\phi}_c)}\right]v^3. \tag{17}$$

By solving Eqs. (12) and (14) numerically, the linear and cubic coefficients in Eq. (17) can be evaluated and the steady-state velocity of the soliton calculated. An example is shown in Fig. 7 along with results from numerical simulations of Eqs. (1)–(3). The agreement is quite good, even more than three times above threshold.

If a perturbation $\boldsymbol{\Pi}$ is added to Eq. (9), small enough to be considered $O(\varepsilon^3)$, then Eq. (17) is modified to

$$\begin{aligned}\partial_t v=&\frac{(\boldsymbol{\psi}_0,[\mathcal{L}-\mathcal{L}_0]\boldsymbol{\phi}_c)}{(\boldsymbol{\psi}_0,\boldsymbol{\phi}_c)}v+\left[\frac{(\boldsymbol{\psi}_0,\mathbf{n}_3)}{(\boldsymbol{\psi}_0,\boldsymbol{\phi}_c)}+\frac{(\boldsymbol{\psi}_0,\partial_\xi\mathbf{w}_2)}{(\boldsymbol{\psi}_0,\boldsymbol{\phi}_c)}\right]v^3\\ &+\frac{(\boldsymbol{\psi}_0,\boldsymbol{\Pi})}{(\boldsymbol{\psi}_0,\boldsymbol{\phi}_c)}.\end{aligned} \tag{18}$$

Note that, since the order parameter of the system is the soliton velocity, the usual order parameter equations (17) and (18) involve the derivative of the velocity with respect to time, or equivalently, the second derivative with respect to time of the soliton position. There is a superficial resemblance to a Newtonian force law obeyed by a massive particle. Figure 11 shows some snapshots of a moving soliton oscillating in a ''potential'' created by adding a small, Gaussian amplitude modulation to the pump:

$$E_I=E_{I0}[1+A\exp(-x^2/w^2)], \tag{19}$$

where $A=O(\varepsilon^3)$. The periodic motion is in complete contrast with the effect the same perturbation would have on a normally stationary soliton. The equation of motion of the latter in an external perturbation is expected to be first order in time and its behavior a function only of its position [3,4]: it would simply follow the amplitude gradient to a local ex-

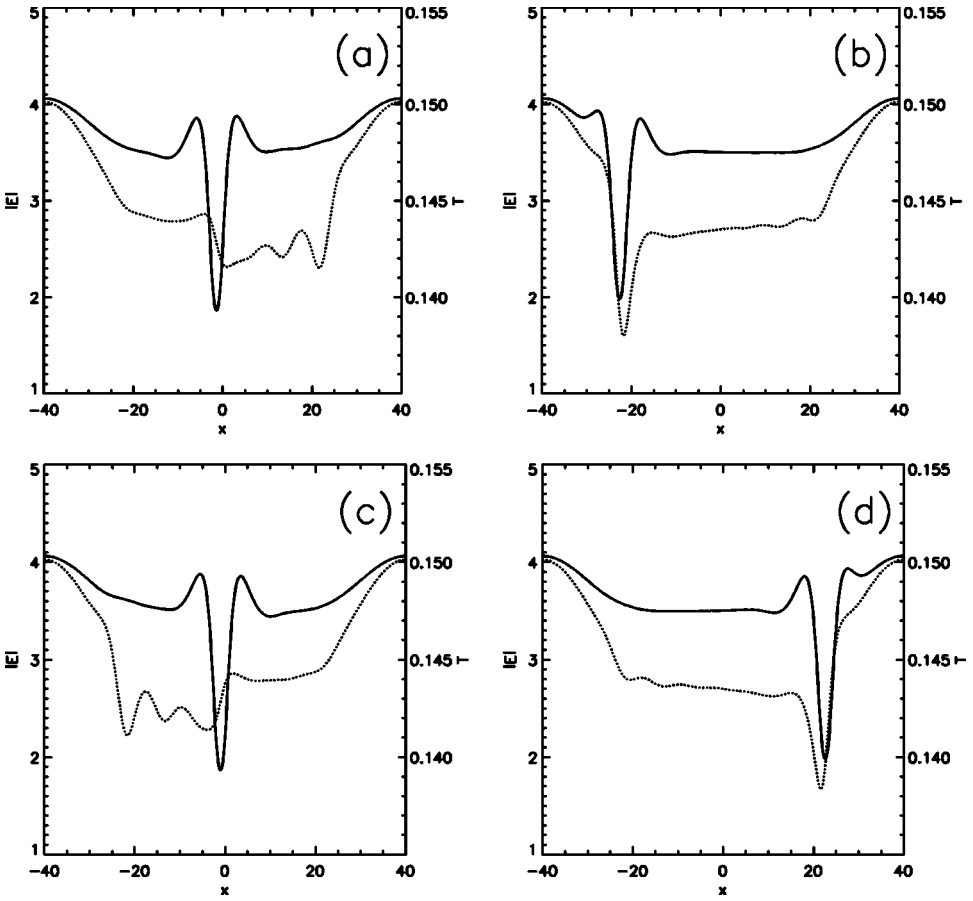

FIG. 11. Dynamical evolution of a dark cavity soliton oscillating in an amplitude-modulated external pump at (a) $t=2.0$, (b) $t=2.7$, (c) $t=3.0$, and (d) $t=3.7$ thermal relaxation times. The solid line shows $|E|$, the modulus of the electric field, while the dotted line is the temperature T. $E_I=5.55$, $\alpha=1$, $A=0.02$, and $w=7.8$. All other parameters as in Fig. 9.

tremum and remain there. An external perturbation drives the velocity of an otherwise stable stationary soliton, while it drives the acceleration of a spontaneously moving soliton.

D. The role of carrier dynamics

In what has been discussed before, we have proposed a mechanism for spontaneous soliton motion which relies on the interplay between the optical field and the lattice temperature. It is natural to ask what role, if any, is played by the carrier dynamics.

The issue can be addressed by ''adiabatically'' eliminating the carrier density from Eqs. (1)–(3). This is done in a nonrigorous way by setting $\partial_t N=0$ (and $D_N\nabla_\perp^2 N=0$) and is intended to represent, loosely, the limit $\gamma_N\to\infty$. For simplicity we neglect radiative recombination of the carriers ($\beta=0$) and therefore set

$$N=\frac{J+|E|^2}{1+|E|^2} \tag{20}$$

to obtain (for an active system)

$$\frac{\partial E}{\partial t}=-(1+i\Theta)E-\Xi\frac{(1-i\Delta)(1-J)}{1+|E|^2}E+E_I+i\nabla_\perp^2 E, \tag{21}$$

$$\frac{\partial T}{\partial t}=-\gamma_T\left[T-Z\frac{(J+|E|^2)}{(1+|E|^2)}-PJ^2-D_T\nabla_\perp^2 T\right]. \tag{22}$$

As with Eqs. (1)–(3), stationary solutions of the above two equations can be calculated, along with their stability properties, and the equations can be integrated in time. By these means, stationary-to-moving transitions have also been identified in Eqs. (21) and (22), as Fig. 12 illustrates. From simulations, the elimination of the carrier dynamics has the effect

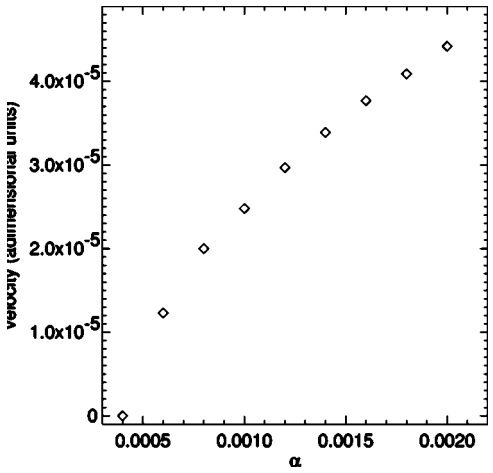

FIG. 12. The velocity of a moving soliton as a function of α. All parameters as in Fig. 4.

of increasing the speed of solitons on a given detuning gradient. Since the soliton cannot respond on a time scale faster than $\min(\gamma_N^{-1},1)$, when the relaxation rate of N becomes very large (in this case infinite), the soliton motion is limited only by the cavity lifetime. For this reason the value of α at the bifurcation point is much smaller in Fig. 12 than in Fig. 7 (the solitons are much more sensitive to temperature gradients).

The analysis of Eqs. (21) and (22) supports our assertion that the motional instability is due essentially to the interaction between the optical and thermal fields. In addition, Eqs. (21) and (22) provide a simpler model with which to examine the moving solitons than Eqs. (1)–(3). Variations on such reduced, two-equation models are therefore the focus of current work.

IV. TWO-DIMENSIONAL MOVING CAVITY SOLITONS

We have verified the existence of moving solitons in two spatial dimensions, as Fig. 13 shows. The existence of a continuum of moving solitons, one for each direction in space, allows complicated and interesting interactions, such as soliton-soliton scattering. In Fig. 13 two solitons with a small transverse displacement approach each other (a) and, when they are close enough, the diffraction ripples around each soliton exert forces which cause them to rotate around their midpoint (b). As the temperature profile changes in response to the orbiting solitons, their orbital speed slows and reverses (c). Finally the force exerted by the temperature gradient forces the solitons apart once more but in directions different from those of their initial velocities (d).

A more detailed study of the interactions between moving solitons will be reported elsewhere.

V. CONCLUSIONS

We have demonstrated the existence, in both one and two spatial dimensions, of spontaneously moving cavity solitons in a model of a semiconductor microcavity. These solitons appear through an instability of the stationary solitons arising from localized temperature changes in the semiconductor. The existence of this straightforward physical interpretation of the motional instability is a particularly appealing feature of the model. Regardless of the details of the present system, however, the essential ingredients appear to be the existence of stationary soliton solutions and the spontaneous creation of ''parameter'' gradients. We therefore expect moving solitons to be present in a wide range of optical and other systems.

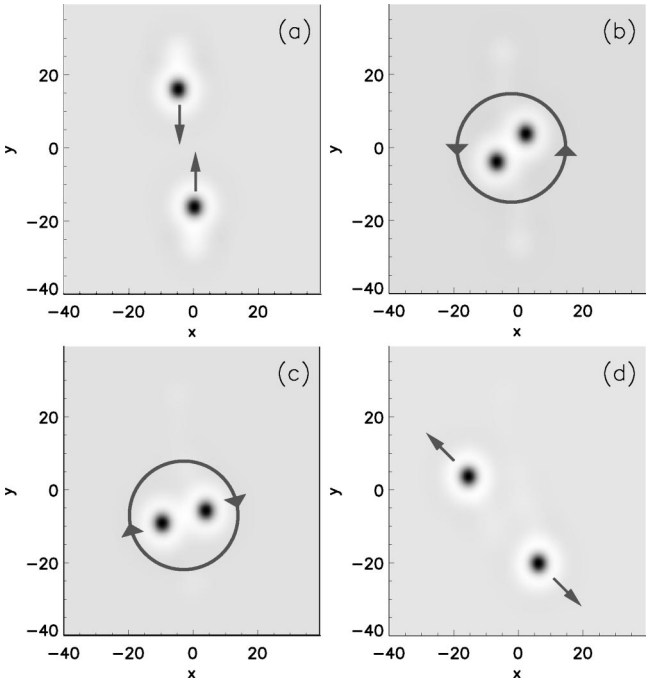

FIG. 13. Dynamical evolution of two-dimensional colliding dark cavity solitons with arrows indicating directions of motion. Snapshots of the modulus of the electric field at (a) $t=0.15$, (b) $t=1.0$, (c) $t=2.0$, and (d) $t=2.75$ thermal relaxation times. Parameters are $E_I=5.55$ and $\alpha=1$. All other parameters as in Fig. 9.

ACKNOWLEDGMENTS

The authors acknowledge financial support from EPSRC Grants No. GR/M 31880 and No. GR/M 19727, and ESPRIT LTR Project No. 28235 (PIANOS) [17]. Finally we would like to thank fellow partners within the PIANOS collaboration for access to results prior to publication, especially the authors of Ref. [5].

[1] W.J. Firth, in *Soliton-Driven Photonics*, edited by A.D. Boardman and A. P. Sukhorukov (Kluwer Academic, London, 2001), pp. 459–485.
[2] W.J. Firth and C.O. Weiss, Opt. Photonics News **26**, 54 (2002).
[3] W.J. Firth and A.J. Scroggie, Phys. Rev. Lett. **76**, 1623 (1996).
[4] T. Maggipinto, M. Brambilla, G.K. Harkness, and W.J. Firth, Phys. Rev. E **62**, 8726 (2000).
[5] L. Spinelli, G. Tissoni, L. Lugiato, and M. Brambilla, Phys. Rev. A (to be published).
[6] P. Coullet, J. Lega, B. Houchmanzadeh, and J. Lajzerowicz, Phys. Rev. Lett. **65**, 1352 (1990).
[7] D. Michaelis, U. Peschel, F. Lederer, D.V. Skryabin, and W.J. Firth, Phys. Rev. E **63**, 066602 (2001).
[8] D.V. Skryabin, A. Yulin, D. Michaelis, W.J. Firth, G.-L. Oppo, U. Peschel, and F. Lederer, Phys. Rev. E **64**, 056618 (2001).
[9] L. Spinelli, G. Tissoni, M. Brambilla, F. Prati, and L. Lugiato, Phys. Rev. A **58**, 2542, (1998).
[10] L. Spinelli, G. Tissoni, M. Tarenghi, and M. Brambilla, Eur. Phys. J. D **15**, 257 (2001).
[11] C. Degen, I. Fischer, W. Elsser, L. Fratta, P. Debernardi, G.P. Bava, M. Brunner, R. Hvel, M. Moser, and K. Gulden, Phys. Rev. A **63**, 023817 (2001).
[12] I. Ganne, G. Slekys, I. Sagnes, and R. Kuszelewicz (unpublished).

[13] T. Rossler, R.A. Indik, G.K. Harkness, J.V. Moloney, and C.Z. Ning, Phys. Rev. A **58**, 3279 (1998).
[14] W.H. Press, S.A. Teukolsky, W.T. Vetterling, and B.P. Flannery, *Numerical Recipes—The Art of Scientific Computing*, 2nd ed. (Cambridge University Press, Cambridge, 1993).
[15] G.-L. Oppo, A.J. Scroggie, and W.J. Firth, Phys. Rev. E **63**, 066209 (2001).
[16] G. Iooss and D.D. Joseph, *Elementary Stability and Bifurcation Theory* (Springer-Verlag, New York, 1980).
[17] Processing of Information by Arrays of Nonlinear Optical Solitons homepage, www.pianos-int.org